Contribution of the Loss of Nanocrystal Ligands to Interdot Coupling in Films of Small CdSe/1-Thioglycerol Nanocrystals

Dae I. Kim,[†] Mohammad A. Islam,[†] Luis Avila,[‡] and Irving P. Herman*[,†]

Materials Research Science and Engineering Center, Department of Applied Physics and Applied Mathematics and Department of Chemistry, Columbia University, New York, New York 10027

Received: February 7, 2003

The broadening of the exciton absorption peak in films composed of small, ∼2 nm diameter CdSe nanocrystals capped by 1-thioglycerol has been interpreted as evidence of interdot carrier coupling. This exciton broadening is seen here for 2.1 nm diameter CdSe nanocrystal arrays, and part of it is correlated with the loss of over half of the 1-thioglycerol molecules from the nanocrystal surfaces. These ligands are even more weakly bound in films of 4.1 nm diameter particles, as evidenced by the smaller shift in their ∼2560 cm^{-1} S−H stretching peak and the faster decay of this peak vis-à-vis that of the smaller particles, but no exciton broadening is observed for these films.

Introduction

The synthesis of II−VI and III−V semiconductor nanocrystals has been pioneered by Alivisatos and co-workers,[1,2,3] Bawendi and co-workers,[4,5,6] and others, who have also detailed the remarkable size-dependent optical,[7] mechanical,[8] and electronic[9] properties of these individual nanoparticles. Moreover, the ability to form novel arrays of these nanoparticles is equally intriguing, in part due to the potential for collective behavior in such arrays.

Semiconductor,[10,11] metal,[12,13] metal oxide,[14] and magnetic[15] nanoparticles have been self-assembled to make quantum dot superlattices. Coupling of carriers between the dots in such ordered and in disordered nanocrystal arrays is not very well understood, particularly for arrays of semiconductor dots; coupling between metal dots has been demonstrated more definitively.[12] The ligands[4,16] that passivate semiconductor nanocrystals and sterically stabilize them in solution usually create a large potential barrier between neighboring dots, which confines carriers within the individual dots. Still, there is some evidence of interdot coupling in arrays of semiconductor nanocrystals. Artemyev et al.[17,18] suggested that there is interdot coupling of carriers in close-packed arrays of 1.8 nm diameter CdSe nanoparticles that are capped by 1-thioglycerol (TG), partly on the basis of the observed broadening and small red shift in the first exciton absorption band; such evidence for coupling was not seen for larger dots. The studies of CdSe nanocrystal films at high pressure by Kim et al.[19] provided some evidence of coupling at elevated pressure, but this evidence was not definitive. Dollefeld et al.[20,21] investigated the particle−particle interaction in dry cast films and crystalline arrays of $Cd_{17}S_4(SCH_2CH_2OH)_{26}$ and $Cd_{32}S_{14}(SCH_2CH(CH_3)OH)_{36}$ cluster compounds. They saw evidence for coupling in the crystalline arrays, but also noted that citing the shift in the exciton peak frequencies in transmission experiments between nanoparticle solutions and arrays as evidence for interdot coupling can be misleading because of polarization effects at high dot density and scattering. Recently, Micic et al.[22] reported coupling in arrays of small InP quantum dots.

Since the properties of the ligands that cap these nanocrystals critically affect such coupling, their stability is important. Kim et al.[23] used attenuated total reflection (ATR) infrared (IR) spectroscopy to follow the pyridine ligands on 3.0 nm diameter CdSe nanoparticles, while close-packed disordered arrays were made from these dots, dispersed in pyridine, as the solvent dried. In forming ∼1-μm thick (300 monolayer) arrays, only ∼30% of the pyridine ligands remained bound after 3 days; in thinner arrays an even smaller fraction remained bound. The broadening of the absorption exciton peaks in arrays of 3.3 nm diameter CdSe dots capped by pyridine seen by Kim et al.[19] at high pressure was attributed to possible contact between semiconductor cores as a result of the loss of most pyridine ligands during film formation.

The current study compares the evolution of the exciton absorption spectrum and the infrared absorption of ligands during the formation of arrays of CdSe nanocrystals capped by TG as the films dry, in the context of the stability of these ligands used in ref 18. The results indicate that much of the interdot coupling observed for small (∼2 nm diameter) CdSe nanocrystals is the result of the loss of a substantial fraction of these TG ligands.

Experimental Procedure

CdSe nanocrystals with 2.1 nm ("small dots") and 4.1 nm ("large dots") semiconductor core diameters and capped by *n*-trioctylphosphine oxide (TOPO) [called CdSe/TOPO dots] were synthesized according to the method of Murray et al.[4] To prepare CdSe/TG dots, these TOPO ligands were replaced by pyridine by refluxing the particles with excess pyridine for ∼10 h at 80 °C and then again at 100 °C,[18] and then the pyridine ligands were replaced by 1-thioglycerol by adding the thioglycerol dropwise, leaving the particles overnight at room temperature; this was followed by the addition of pyridine and then ultrasonication to redissolve the particles.[18] Disordered, ∼1-μm thick arrays were formed by placing a drop of solution of CdSe/TOPO dots dissolved in hexane or CdSe/TG dots dissolved in pyridine and letting the solvent evaporate at room

* Corresponding author: E-mail: iph1@columbia.edu.
[†] Department of Applied Physics and Applied Mathematics.
[‡] Department of Chemistry.

10.1021/jp030168h CCC: $25.00
Published on Web 06/05/2003

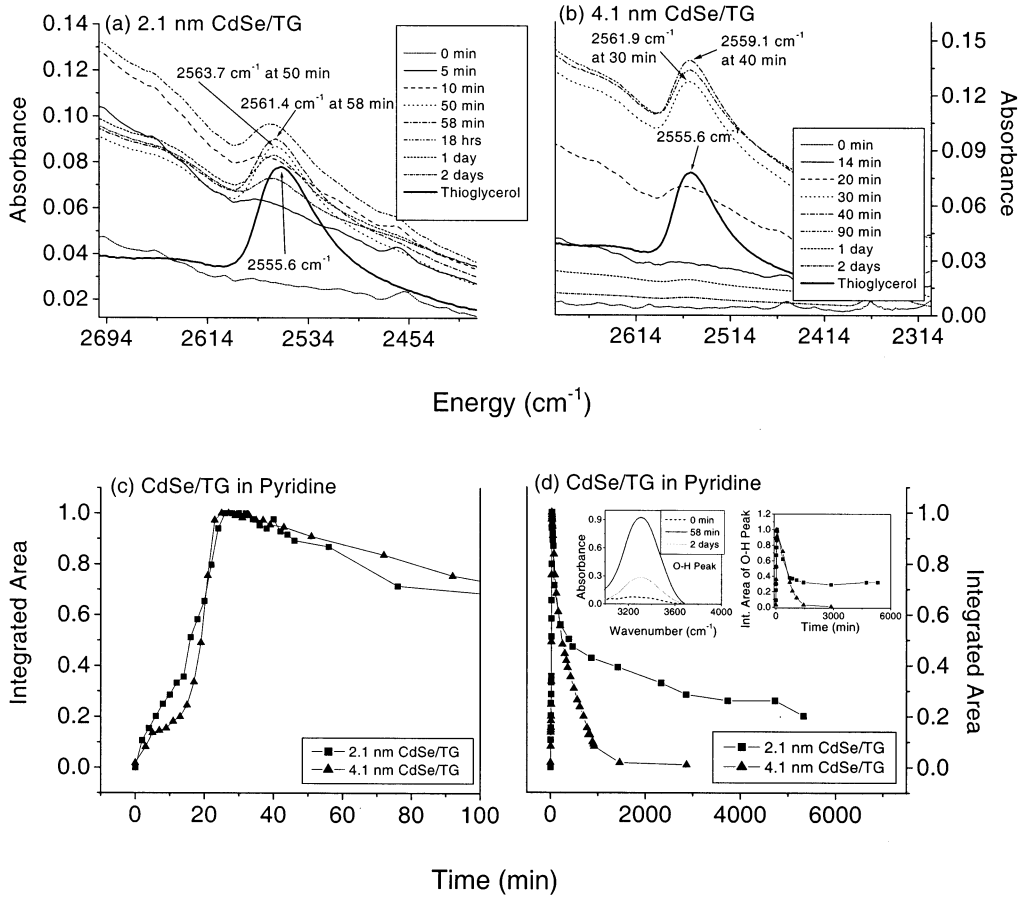

Figure 1. Absorbance near the ~2560 cm^{-1} S−H stretching peak in TG is followed during the drying (a) 2.1 nm diameter and (b) 4.1 nm diameter CdSe/TG nanocrystal films in pyridine solvent and compared to that for neat 1-thioglycerol, along with the integrated area of this peak for (c) shorter- and (d) longer-term drying times. The left inset to Figure 1(d) shows the absorbance of the O−H peaks of the TG ligand for the 2.1 nm diameter dots at selected times (those for the 4.1 nm diameter dots are not shown). The right inset shows the integrated area of this peak for both the 2.1 and 4.1 nm diameter dots as a function of drying time.

temperature. (Significant room-temperature exchange of pyridine with TG can be ignored, as is shown below.) The samples were stored in a drybox under Ar gas flow to prevent possible oxidation when data was not being collected.

Visible absorption spectroscopy was used to follow the electronic properties of these films drying on coverglass substrates; all times are referenced to when the solution was dropped to form the film. The dried films were 1.1 μm thick for the 2.1 nm particles and 1.4 μm thick for the 4.1 nm particles, as measured by profilometry. Film thickness across these relatively slowly drying films was within ±10%. Measurements (5-s traces) began ~8 min after drying began, when the films dried sufficiently for the coverglass to be vertical ("minimally" dried film). Absorption spectra were periodically collected.

Multireflection ATR spectroscopy utilizing a ZnSe GRASEBY-SPECAC horizontal ATR accessory mounted on a Perkin-Elmer PE-1000 Paragon Fourier transformed infrared (FTIR) spectrometer was used to follow the solvent and ligands during the formation of the films (16 s per spectrum). Initially, the solution forms a ~100−120 μm thick film and dries to a ~1.05 μm thick film in about an hour, as seen below.

Film thickness was measured by profilometry on other substrates under the same conditions: area, etc., since it could not be measured directly on the ZnSe prism. The visible and ATR absorption spectroscopies probe the entire thickness of the ~1-μm-thick dried films. Initially ATR probes only about a wavelength (~0.78 μm) deep into the solution, but eventually the whole sample is interrogated due the evaporation of the solvent to leave a ~1-μm-thick dried film and the increase of the index of refraction of the film; this is discussed in more detail below.

Once the experiments were finished, the large and small CdSe/TG dot films were redissolved in pyridine solvent by first mixing them with excess TG, adding pyridine, and then ultrasonicating them. The absorption spectra of these nanoparticle solutions were found to be identical to those of the initial solutions used to make the film. This shows that there were no large changes in the dots during film formation (other than those described below), such as due to the oxidation of the surface.

Results

Figure 1 shows the ATR spectrum of the S−H stretch of neat TG and TG dot ligands during drying of CdSe/TG dots in pyridine solvent. The intensity of the 2561.4 cm^{-1} (2.1 nm particles) and 2559.1 cm^{-1} (4.1 nm particles) S−H stretching peak in TG, thought to be involved in the bonding of the TG to the CdSe dot surface, is followed for the drying films. The left inset of Figure 1d shows the evolution of the ~3310 cm^{-1} O−H stretching peak in TG at selected times for the 2.1 nm diameter CdSe/TG dots. The spectra for the 4.1 nm diameter CdSe/TG dots are qualitatively similar, but are not shown. The right inset shows the time dependence of the integrated area of this O−H peak for both the 2.1 and 4.1 nm diameter CdSe/TG dots. The evolution of the 882 cm^{-1} TG S−H bending mode peak also looks the same for both nanocrystal films (not shown). The infrared spectra in the regions of the pyridine peaks for the 2.1

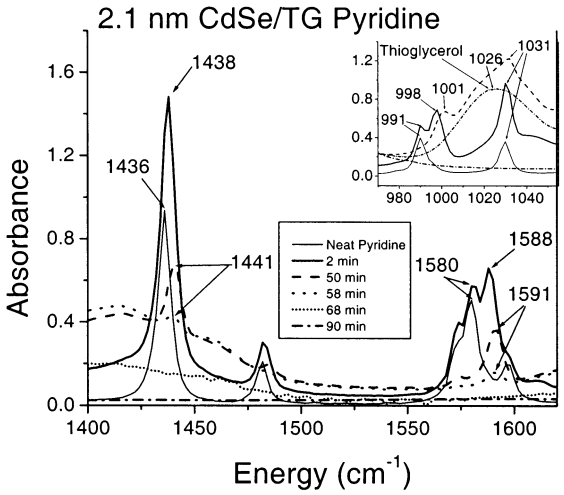

Figure 2. The infrared spectra in the regions of pyridine peaks during the drying of 2.1 nm diameter CdSe/TG nanocrystal films in pyridine solvent and compared to that for neat pyridine.

nm CdSe/TG dots are shown in Figure 2; the results for the 4.1 nm diameter particles are very similar. No changes were seen in the TOPO infrared peaks during the drying of CdSe/TOPO dot films (not shown). The evolution of the first exciton peaks in the visible absorption spectra of the small and large dots capped by TOPO or TG is shown in Figure 3 for these films.

Discussion

In neat thioglycerol the S−H stretching vibration is at 2555.6 cm^{-1} (Figure 1). Initially (0 min) this S−H peak from the ligands is not seen because of the low concentration of dots in the probed region near the surface. For the 2.1 nm particles, this peak appears at 2563.7 cm^{-1} at 50 min (when much of the solvent has evaporated) and at 2561.4 cm^{-1} at 58 min (when virtually all of the solvent has evaporated), and are upshifted by ∼8 cm^{-1} and ∼6 cm^{-1} relative to the neat TG. For the 4.1 nm particles they appear at 2561.9 cm^{-1} at 30 min and 2559.1 cm^{-1} at 40 min, upshifted by 6.3 and 3.5 cm^{-1}. TG is not used as the solvent during film formation since the solvent and the ligand peaks could not then be resolved to differentiate between solvent and ligand stability because of these small shifts. There is consistently a larger upshift in the smaller dot, suggesting that TG is more strongly bound to these dots.

The number of nanocrystals probed by ATR varies with time and depends on the exponential penetration depth of the IR beam,[24] which is $\lambda/2\pi(\sin^2\theta - n_{21}^2)^{1/2}$ where θ is the incident angle, $n_{21} = n_2/n_1$, $\lambda = \lambda_{vacuum}/n_1$ (λ is the wavelength in the prism), n_1 is the refractive index of the ZnSe prism (2.43 at 3.9 μm of the TG peak), and n_2 is the refractive index of the drying film. θ is fixed at 45° by the prism and coupling geometry. At this angle, internal reflection occurs when the external media has $n_2 \leq 1.7$. The beam reflects ∼6−7 times from the surface covered with the array, and this does not change much during

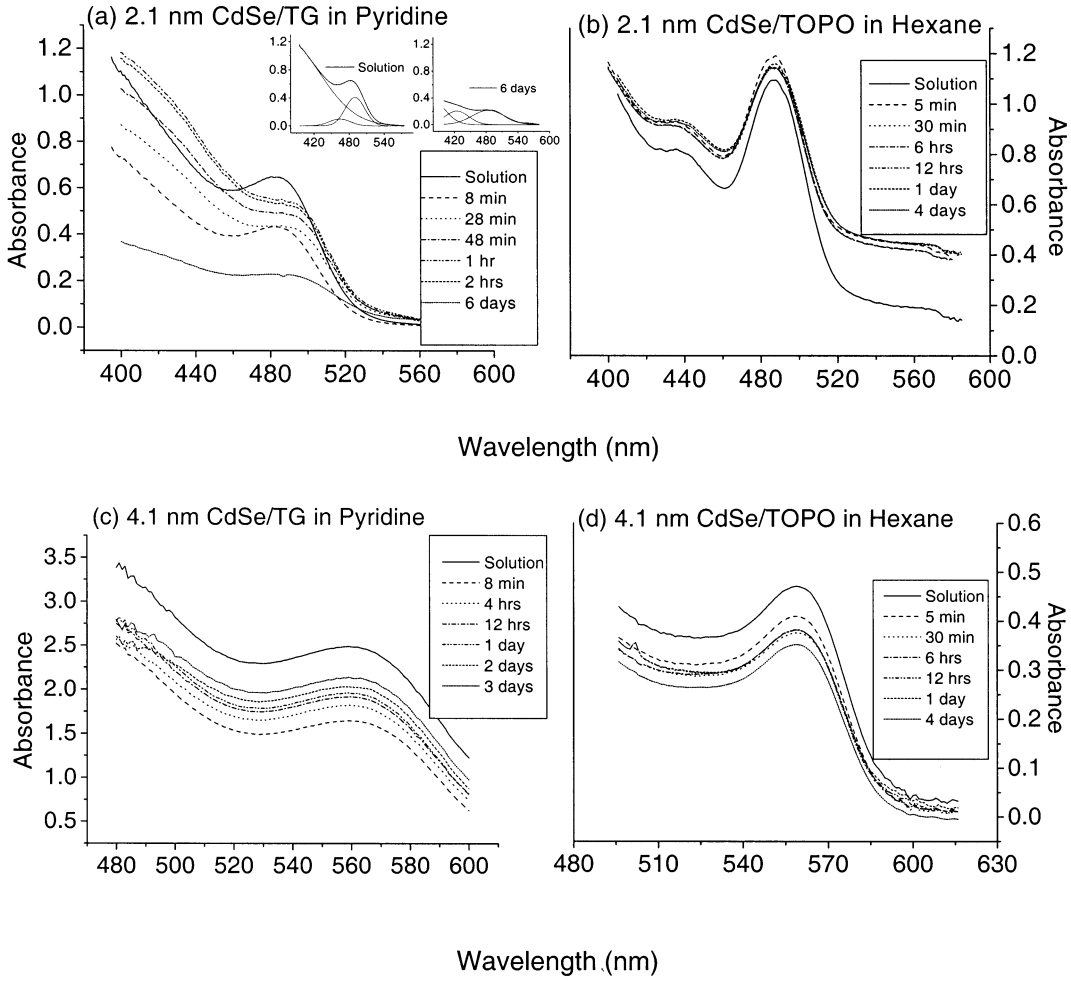

Figure 3. The evolution of the visible absorption spectrum during drying of films composed of 2.1 nm diameter CdSe nanocrystals capped by (a) TG in pyridine solvent and (b) TOPO in hexane solvent, and 4.1 nm diameter CdSe nanocrystals capped by (c) TG in pyridine solvent and (d) TOPO in hexane solvent, along with the spectra of the nanocrystals in solution. Not all taken spectra are shown. The insets to (a) show the Gaussian profile fit of the first exciton peak.

drying. Right after the nanocrystal solution drop is placed on the ZnSe prism, the IR beam probes about 0.2 λ or ~0.78 μm into the solvent (using $n_2 \approx n_{\text{pyridine}} = 1.507$ at 3.9 μm) and it probes a very low density of nanoparticles (cumulatively ~0.7% of the total). As the solvent evaporates, the density of the nanoparticles in the probed region increases and the probe depth increases due to the increasing refractive index of the drying film; both factors account for the initial increase in the bound TG peaks, as seen in Figure 1c. In fact, during solvent evaporation the probe depth (calculated for a semi-infinite external medium) becomes many times the thickness of the film. With no solvent remaining, the effective refractive index of the film exceeds 1.7 and there is no internal reflection at the ZnSe/dot film interface for $\theta = 45°$; the IR beam likely probes the entire depth of the dried array and is totally internally reflected at its outer surface.[25]

The pyridine solvent peak near ~1440 cm^{-1} disappears in ~58 min ("totally" dried film) (Figure 2). The integrated intensities of the S−H stretching peaks in Figure 1 initially increase during this evaporation as more and more of the dots are concentrated in the ever-increasing ATR probe depth, as discussed in the preceding paragraph. After the maximum is reached at ~40 min for the 2.1 nm dots, there is a slow decay of the S−H peak, indicating slow loss of the thioglycerol ligands, with ~25−35% remaining after 3 days of drying; the loss is faster and much more complete for the 4.1 nm dots (Figure 1d). Moreover, the decrease in ligand frequency with time for the small and large dots suggests that some TG ligands are more weakly bound and are lost faster. There is a 10% decrease in the TG peak height from the maximum signal at 25 min to 60 min, suggesting that at least 10% of the TG ligands are lost when the film is totally dried since some could have been lost before 25 min.

These desorbing TG ligands likely leave the film entirely, since any interstitial or surface TG would be observed in the ATR spectra of the dried film. The vapor pressure of TG at room temperature[26] is ~0.01 mmHg. This corresponds to a ~3 μm/s evaporation rate (from liquid TG in an atmosphere with no TG vapor), so TG desorbing from the dots should leave the ~1-μm-thick films (which are only partially TG) very quickly relative to the typical time scales here.

All of the peaks observed for neat TG are also seen for the TG ligands on the nanocrystals, with roughly the same relative intensities. This suggests that the H in the S−H group that is thought to be bound to the nanocrystal surface is not lost when TG binds; this is different from what has been observed when thiols (more strongly) bind to a flat Au surface.[27] Moreover, the intensities of the other ligand vibrational peaks evolve with time as does the intensity of the S−H stretch for both the 2.1 and 4.1 nm diameter dots, as is shown for the 3310 cm^{-1} O−H peak in the inset to Figure 1d. The integrated area of this O−H peak initially increases until the solvent dries completely and then decreases—in 3 days to ~25% of the peak value for the 2.1 nm diameter dots and to nearly zero for the 4.1 nm diameter dots. These time dependences for the 3.9 μm (S−H stretch) and 3.0 μm (O−H stretch) peak intensities were also seen for the S−H bending peak, which confirms that H loss during binding does not appear to be significant. Since the S−H bending peak is at a much longer wavelength 11.3 μm (882 cm^{-1}), limited probe depth in the film and scattering due to any surface roughness are not important, because they would be very dependent on wavelength.

There is also some evidence of pyridine binding to the CdSe core in these CdSe/TG dots. In ref 23, four prominent peaks of pyridine bound to the CdSe dots were followed at 1600, 1445, 1036, and 1010 cm^{-1}, which were, respectively, upshifted by 20, 9, 5, and 19 cm^{-1} relative to the 1580, 1436, 1031, and 991 cm^{-1} peaks in neat pyridine. Figure 2 shows these solvent peaks at 1580, 1438, 1031, and 991 cm^{-1}. After solvent evaporation (after ~58 min), there is a pyridine peak at 1441 cm^{-1} in the 2.1 nm dots, upshifted by 5 cm^{-1} relative to the neat solvent, which is about half the 9.1 cm^{-1} shift for CdSe/pyridine dots measured in ref 23 for 3.0 nm particles. Two additional initial pyridine solvent peaks at 1588 and 998 cm^{-1} are upshifted by ~3 cm^{-1} to 1591 and 1001 cm^{-1}, respectively, as more of the solvent dries. This suggests that there is binding of some pyridine to the surface; however, the binding of these pyridine molecules to the surface sites of CdSe/TG dots is weaker than that in CdSe/pyridine dots. Therefore, there is either bonding of pyridine to sites that are not capped by TG or replacement of TG by pyridine in some surface sites that very weakly bind TG. These peaks decease to almost zero (<1% of the maximum value) in ~90 min. This is much shorter than the tens of hours decay time seen for CdSe/pyridine dots in ref 23, which is also consistent with much weaker binding.

The visible absorption spectra during the drying of CdSe/TOPO dot films (Figure 3) look nearly the same for the small and large dots—aside from the shift in exciton energy. For the 4.1 nm diameter dots, the spectra of the solution and the film are identical; no change with time is seen in the film. (The films of CdSe/TOPO dots in hexane dry in <1 min.) The first exciton peak of the dried film of the 2.1 nm diameter dots also does not change with time; however, it is ~1.1 nm broader than that of the solution (Figure 3b). The unchanging width of the dried dot films is expected since the TOPO ligands on CdSe are known to be stable, as confirmed here by ATR.

Initially, the exciton absorption peaks of the drying CdSe/TG dot films look the same for the small and large dots (Figure 3, parts a and c) − aside from the shift in energy of this first exciton. They both are a bit broader than those for CdSe/TOPO dots; this is not likely due to interdot coupling, and may be due to the effect of these ligands on wave function localization or the refluxing operation. The spectra of the 4.1 nm CdSe/TG dots do not change with time, while those of the 2.1 nm dots become much broader, which is consistent with the observations in ref 18. Even with near total ligand loss, there is no broadening and presumably no interdot coupling in the dried films composed of the large dots.

Figure 4 compares the broadening of the first exciton peak of the 2.1 nm diameter CdSe/TG dot film in Figure 3a (including data not shown in this figure) with the area of the 2561.4 cm^{-1} TG ligand peak in Figure 1d (which is affected by solvent evaporation and TG ligand loss). After solvent evaporation (>30 min), when the IR beam probes the entire film, exciton broadening inversely correlates with the area of the IR peak of the S−H ligand. The fwhm of the first exciton peak plotted here is determined by fitting the absorption spectrum with multiple Gaussian peaks, as illustrated in the insets to Figure 3a. The fwhm of the first exciton peak of the 2.1 nm diameter CdSe/TG dots solution is ~172 meV. (The uncertainties in these widths are ±5−10 meV.) It increases to 207 meV in the minimally dried film (8 min; some solvent remaining, no ligand loss) and to 257 meV after 1 h in the totally dried film (no solvent, at least 10% ligand loss). The fwhm changes slowly after this; it is 299 meV after 1 day (60% ligand loss) and 315 meV after 2 days (70% ligand loss), and then remains constant up to the end of 6 days (Figure 4). Relative to the solution, this exciton peak broadens by 35, 85, 127, and 143 meV after 8

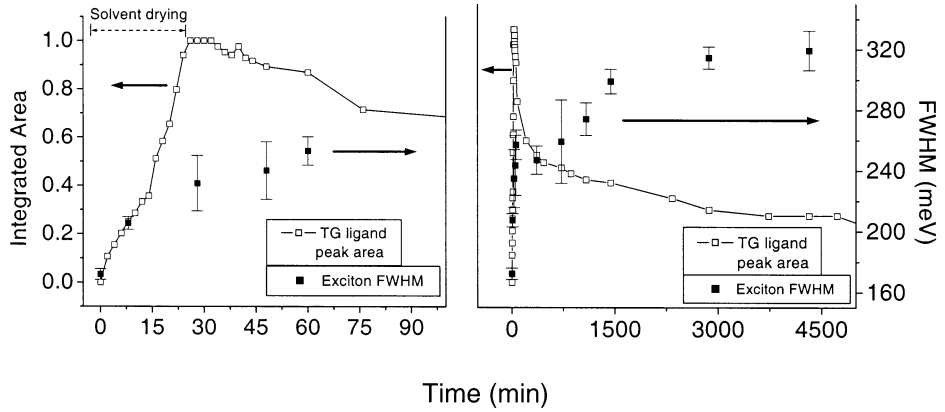

Figure 4. The evolution of the measured line width (fwhm) of the first exciton absorption peak in the drying array of 2.1 nm diameter CdSe/TG nanocrystals in pyridine solvent is compared to that of the normalized integrated area of the ~2561.4 cm^{-1} S−H stretching peak in the TG ligands.

min, 1 h, 1 day, and 2 days, respectively. Assuming Gaussian inhomogeneous broadening in the solution and a Gaussian band broadening mechanism, after deconvolution the fwhm of the exciton broadening contribution would be 115, 191, 245, and 264 meV, respectively, at these four times. [The previous set of broadening numbers (simple differences) corresponds to Lorentzian broadening for both the initial inhomogeneous distribution and exciton broadening.] The degree of exciton broadening is bracketed by these two numbers, e.g., between 143 and 264 meV after 2 days.

Some of the broadening is likely associated with solvent evaporation, but much of it is clearly due to the loss of ligands. Both processes bring the dots closer together. At 1 h, there is no solvent throughout the film, but at least 10% of the ligands are missing also. Note that the entire thickness of the film is being probed in the infrared and ultraviolet as discussed earlier in this section, and drying is not likely to be uniform; the top loses solvent and dries before the bottom, and it loses ligands before the bottom.[23]

Reference 18 suggested that interdot coupling occurs only between small CdSe/TG dots, and that the mechanism is by tunneling through the ligand barriers—and not by conduction through ligands. Wave function delocalization leading to coupling between dots is enhanced for smaller effective masses, shorter distances between the surfaces of the semiconductor cores, and for smaller cores—for which wave function leakage outside the core is larger for isolated dots. Using known bulk valence and conduction band offsets[28] and effective masses,[29] wave function leakage may be largest for electrons. (For CdSe, the effective mass of the electron is 0.12 m_0 and that of the hole is 0.41 m_0, where m_0 is the mass of a free electron.[29]) Figure 5 shows the total width of this conduction band for 0.5 and 1.0 eV barriers between the 2.1 or 4.1 nm CdSe dot cores, as a function of separation of the dot cores d expected from a 1 D Kronig-Penney model[30] (electron effective mass 0.12 m_0 in the core—assumed to be equal to that of bulk CdSe[29]—and m_0 outside).

Experimental broadening in the visible absorption spectra, beyond that in the dot solutions, is also plotted in Figure 5, using the loss of ligands to estimate the interdot distance. The final nearest-neighbor separation of the outer core surfaces was determined to be 0.7 nm in ref 4 for tributylphosphine oxide and pyridine ligands on 3.3 nm CdSe dots.[31] These ligands are roughly comparable in size to TG, and so the interdot separations in the 2.1 and 4.1 nm CdSe/TG dot films are assumed to be 0.7 nm here. The interdot distance d is assumed to depend on the fraction of remaining TG ligands f in two very different ways.

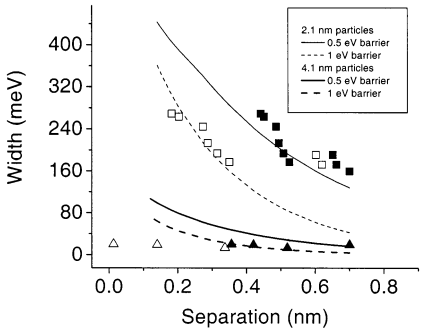

Figure 5. The total band broadening line width from the Kronig-Penney model for the 2.1 and 4.1 nm particles, assuming 0.5 and 1.0 eV barriers vs interdot separation of the CdSe core surfaces, is compared to the Gaussian fwhm of the first exciton peak for the 2.1 nm (squares) and 4.1 nm (triangles) diameter particles capped by TG after deconvoluting the measured profile from that of the exciton for the dots in solution. The core separations for the experimental data are determined from the fraction of remaining TG ligands f from Figure 1, assuming it is either 0.7 nm f (open symbols) or 0.7 nm $(1 + f)/2$ (filled symbols). The open and filled symbols for each particle overlap for 0.7 nm separation.

The fastest possible variation assumes that the distance between dots is proportional to the total number of ligands, as $d = 0.7$ nm f. This would be reasonable if all of the ligands totally resided between two opposing parallel surfaces. Since the surfaces are not flat and part of the molecules are likely squeezed into interstitial regions[32] a slower variation, such as $d = 0.7$ nm $(1+ f)/2$, is likely more realistic.

One would not expect perfect agreement between the model and experiment, given that this Kronig-Penney model only approximates broadening of levels in a 3D structure of a disordered array of near-spherical dots (and likely underestimates it). Also, in Figure 5 the total model bandwidths are compared to the fwhm exciton widths. Still, the data for the 2.1 nm dot films are consistent with ~0.5 eV−1.0 eV high barriers. The slower scaling for interdot separation $d = 0.7$ nm $(1+ f)/2$ seems also to be consistent with observations, giving credence to the importance of ligand loss. The CdSe/TG dots in ref 18 were a bit smaller (1.8 nm) than the small dots here and were synthesized by a different procedure. This could mean that the CdSe core termination and binding to TG are different in ref 18 and the current study. Experiment and modeling here show little exciton broadening for the 4.1 nm dot films for these parameters, which is consistent with expectations from ref 18.

The exciton peaks in the 2.1 nm CdSe/TOPO dot films are broader than that in solution (161 meV) by 5.5 meV, which corresponds to exciton broadening of 43 meV using Gaussian

deconvolution, so ~5−40 meV band broadening is possible. The Kronig-Penney model predicts 53 meV (0.5 eV barrier) and 10 meV (1.0 eV) band broadening for 2.1 nm CdSe dots separated by the 1.1 nm distance expected after drying.[32] This suggests that there might be a little interdot coupling even in these small CdSe/TOPO dot films.

Dollefeld et al.[20,21] found a small red shift in the exciton peak of drycast films of $Cd_{17}S_4(SCH_2CH_2OH)_{26}$ (1.4 nm diameter, 18 meV) and $Cd_{32}S_{14}(SCH_2CH(CH_3)OH)_{36}$ (1.8 nm diameter, 12 meV) cluster compounds relative to that in solution; no additional broadening was seen in either case. For crystal compounds formed of these clusters, there was an even larger exciton red shift (~150 meV) and much exciton broadening (520 meV fwhm) relative to the dot solution (390 meV). They argued that the red shift is a result of higher packing density of the dots, leading to interactions between the transition dipole of the excited dot and the dipole induced in a nearby dot, and scattering. In contrast, they concluded that the broadening is caused by quantum mechanical tunneling of electrons, with a tunneling probability dependent on both the interparticle distance and the tunnel barrier. No red shift during drying is seen in the current study, only exciton broadening. Changes in scattering should be small after solvent evaporation. The model in the current study assumes a tunnel barrier height that is intimately connected to the nature of the ligands and an interparticle distance that depends on the number of ligands remaining on the dots.

It is possible that the binding of sulfur atoms in TG ligands to surface Cd alters the CdSe nanocrystal absorption as would adding a fraction of a monolayer of a CdS shell to a CdSe core. Peng et al.[2] have shown that adding CdS shells to CdSe nanocrystals slightly broadens the absorption exciton feature and shifts it to lower energy. If the loss of some TG ligands simulated the loss of part of the CdS shell, the exciton peak would be expected to narrow and shift to higher energy, neither of which is seen here. In any case, the weak binding of the TG ligands to the CdSe core suggests that the sulfur atoms in TG are more weakly coupled to the core, structurally and optically, than those from a CdS shell would be.

Conclusions

About two-thirds of the 1-thioglycerol ligands are lost on 2.1 nm diameter CdSe/1-thioglycerol nanocrystals during drying of the array, and an even larger fraction is lost for the 4.1 nm diameter dot films. Even after ligand loss, these films are easily redissolved into solution, and these solutions have the same visible absorption spectra as the starting nanocrystal solutions. Rapid interdot coupling does not occur in dried films of the larger dots even with their greater ligand loss, likely because of the small wave function leakage outside the core. Exciton broadening, likely due to wave function delocalization, is seen here for the smaller dots. Part of it may result from solvent loss, even with little loss of ligands, but much of it is clearly caused by the loss of ligands that brings the dots much closer together, enabling interdot tunneling; some contact between the semiconductor cores is also possible.

Acknowledgment. This work was supported primarily by the MRSEC Program of the National Science Foundation under Award Numbers DMR-9809687 and DMR-0213574. The authors thank Michael Steigerwald for valuable conversations.

References and Notes

(1) Peng, X.; Wickham, J.; Alivisatos, A. P. *J. Am. Chem. Soc*. **1998**, *120*, 5343.

(2) Peng, X.; Schlamp, M. C.; Kadavanich, A. V.; Alivisatos, A. P. *J. Am. Chem. Soc.* **1997**, *119*, 7019.

(3) Li, L.; Hu, J.; Yang, W.; Alivisatos, A. P. *Nanoletters* **2001**, *1*, 349.

(4) Murray, C. B.; Norris, D. J.; Bawendi, M. G. *J. Am. Chem. Soc*. **1993**, *115*, 8706.

(5) Dabbousi, B. O.; Rodriguez-Viejo, J.; Mikulec, F. V.; Heine, J. R.; Mattousi, H.; Ober, R.; Jensen, K. F.; Bawendi, M. G. *J. Phys. Chem.* **1997**, *101*, 9463.

(6) Danek, M.; Jensen, K. F.; Murray, C. B.; Bawendi, M. G. *Appl. Phys. Lett*. **1994**, *65*, 2795.

(7) Norris, D. J.; Bawendi, M. G. *Phys. Rev. B* **1996**, *53*, 16338.

(8) Tolbert, S. H.; Alivisatos, A. P. *J. Chem. Phys*. **1995**, *102*, 4642.

(9) Banin, U.; Lee, C. J.; Guzelian, A. A.; Kadavanich, A. V.; Alivisatos, A. P.; Jaskolski, W.; Bryant, G. W.; Efros, Al. L.; Rosen, M. *J. Chem. Phys.* **1998**, *109*, 2306.

(10) Murray, C. B.; Kagan, C. R.; Bawendi, M. G. *Science* **1995**, *270*, 1335.

(11) Motte, L.; Billoudet, F.; Lacaze, E.; Douin, J.; Pileni, M. P. *J. Phys. Chem.* **1997**, *101*, 138.

(12) Collier, C. P.; Saykally, R. J.; Shiang, J. J.; Henrichs, S. E.; Heath, J. R. *Science* **1997**, *277*, 1978.

(13) Giersig, M.; Mulvaney, P. *Langmuir* **1993**, *9*, 3408.

(14) Yin, J. S.; Wang, Z. L. *Phys. Rev. Lett.* **1997**, *79*, 2570.

(15) Sun, S.; Murray, C. B.; Weller, D.; Folks, L.; Moser, A. *Science* **2000**, *287*, 1989.

(16) Peng, X.; Manna, L.; Yang, W.; Wickham, J.; Scher, E.; Kadavanich, A. V.; Alivisatos, A. P. *Nature* **2000**, *404*, 59.

(17) Artemyev, M. V.; Bibik, A. I.; Gurinovich, L. I.; Gaponenko, S. V.; Woggon, U. *Phys. Rev. B* **1999**, *60*, 1504.

(18) Artemyev, M. V.; Woggon, U.; Jaschinski, H.; Gurinovich, L. I.; Gaponenko, S. V. *J. Phys. Chem.* B **2000**, *104*, 11617.

(19) Kim, B. S.; Islam, M. A.; Brus, L. E.; Herman, I. P. *J. Appl. Phys.* **2001**, *89*, 8127.

(20) Dollefeld, H.; Weller, H.; Eychmuller, A. *J. Phys. Chem. B* **2002**, *106*, 5608.

(21) Dollefeld, H.; Weller, H.; Eychmuller, A. *Nanoletters* **2001**, *1*, 267.

(22) Micic, O. I.; Ahrenkiel, S. P.; Nozik, A. J. *Appl. Phys. Lett*. **2001**, *78*, 4022.

(23) Kim, B. S.; Avila, L.; Brus, L. E.; Herman, I. P. *Appl. Phys. Lett*. **2000**, *76*, 3715.

(24) Harrick, N. J.; duPre, F. K. *Appl. Opt.* **1966**, *5*, 1739.

(25) An effective medium theory with volume averaging of dielectric constants, $\epsilon_{CdSe} = 9.7$, $\epsilon_{TG} = 2.33$, and $\epsilon_{pyridine} = 2.27$ at 3.9 μm, is used to determine the refractive index of the film. It assumes fcc close packing of the nanocrystals with 74% packing density, capped by TG, and the pyridine solvent filling the interstitial regions. This assumes that the interdot spacing is 0.7 nm. When there are equal densities of bound TG on the 2.1 nm diameter nanoparticles and free pyridine in the interstitial regions, the film refractive index is 2.14. When all of the pyridine solvent is gone and all of the TG capping remains, the refractive index is 2.10; with only 30% of the capping TG remaining, it is ~1.96, assuming the interdot spacing does not change. (If the interdot spacing does change, as described in the text and in Figure 5 as $d = 0.7\ (1 + f)/2$, then for 30% of the ligands remaining and with no pyridine the index of refraction is 2.22.) In any event since $n_{film} > 1.7$, there is no internal reflection at the ZnSe/film interface for $\theta = 45°$ and the IR beam likely probes the entire depth of the dried array and is totally internally reflected at its outer surface. Even if these estimates of refractive index are a bit high, the penetration depth still increases to way beyond the actual film thickness.

(26) This ~0.01 mmHg TG vapor pressure at room temperature is estimated using the 5 mmHg vapor pressure at 118 °C (Lewis, R. J., Sr. *Hazardous Chemicals Desk Reference*, 3rd ed.; Van Nostrand: New York, 1993; p 895) and the room-temperature vapor pressure for other organics with the same vapor pressure at this higher temperature (Stull, D. R. *Ind. Eng. Chem.* **1947**, *39*, 517). This gives a range of 0.005−0.014 mmHg. The conclusion that TG is sufficiently volatile to leave the film fast on the observed times scales is valid for any vapor pressure in this range.

(27) Laibinis, P. E.; Whitesides, G. M.; Allara, D. L.; Tao, Y.-T.; Parikh, A. N.; Nuzzo, R. G. *J. Am. Chem. Soc*. **1991**, *113*, 7152.

(28) Wie, S.; Zunger, A. *Appl. Phys. Lett.* **1998**, *72*, 2011.

(29) Lippens, P. E.; Lanoo, M. *Phys. Rev. B* **1990**, *41*, 6079.

(30) Kronig, R. *Band Spectra and Molecular Structure*; The University Press: Cambridge, England, 1930.

(31) The length of a 1-thioglycerol ligand molecule is ~7.6 Å, calculated from the known lengths of the C−C (1.54 Å), C−H (1.09 Å), S−C (1.81 Å), and S−Cd (2.4 Å) bonds and the tetrahedral bond angle (109°). Since the alkane chains of neighboring dots greatly interdigitate and may not be normal to the surface, the core separation is estimated to be ~7 Å.[32] This is used as the interdot distance d in Figure 5 before loss of capping ligands.

(32) Murray, C. B. Ph.D. Thesis, Massachusetts Institute of Technology, 1993.